

# A COMPARATIVE STUDY OF LES COMBUSTION MODELS FOR PREMIXED TURBULENT COMBUSTION

**Christer Fureby**

Dept. of Weapons and Protection, Weapons and Protection  
The Swedish Defense Research Agency, FOI, S-172 90, Stockholm, Sweden  
fureby@foi.se

**Fernando F. Grinstein**

Laboratory for Computational Physics and Fluid Dynamics  
Naval Research Laboratory, Washington DC, 20375-5344, USA  
grinstein@lcp.nrl.navy.mil

**Suresh Menon**

School of Aerospace Engineering  
Georgia Institute of Technology, Atlanta, GA, 30332-0150, USA  
suresh.menon@ae.gatech.edu

**Henry Weller**

Nabla Ltd.,  
The Mews, Picketts Lodge, Salfords, Surrey RH1 5RG, UK  
H.Weller@Nabla.co.uk

## ABSTRACT

The aim of this study is to compare three different state-of-the-art Large Eddy simulation (LES) combustion models for a reactive turbulent mixing layer. The models selected are the Flame-Wrinkling (FW) model, a Monotone Integrated LES (MILES) model in conjunction with global chemistry, and the Linear Eddy Model (LEM). The models are briefly described before results obtained from a computational investigation of a reactive turbulent mixing layer are presented and compared with experimental data. Finally, a discussion is provided concerning the intrinsic natures and capabilities of these models.

## INTRODUCTION

Combustion plays an important role in many engineering applications, as well as in everyday life. The complex phenomenon of combustion is the subject of continual research efforts aiming at better understanding and improved fuel economy. One aspect is the search for computational models to describe the physics involved. Engineering models usually combine Reynolds Average Numerical Simulation (RANS) models of the flow, (Jones, 1993), with combustion models like the Eddy Breakup (EBU), Bray-Moss-Libby (BML), (Bray and Libby, 1994), or Probability Density Function (PDF) models, (Dopazo, 1994). The restricted information provided by RANS about the flow and the combustion model about the combustion physics and the interactions taking place between the flow and the chemistry, preclude accurate prediction of cycle-to-cycle variations and com-

bustion induced instabilities associated with unsteady vortex dynamics, which are crucial for active and passive control of the flow and combustion. Alternatively, Large Eddy Simulation (LES) is attractive as it provides a compromise between accuracy and cost and is presently considered a practical approach for engineering applications. The key feature of LES is that it attempts to capture the evolution of the large scale flow at the same time as it allows for inclusion of realistic flow and chemistry parameters. However, the flame-brush thickness  $\lambda_L$  is usually smaller than the affordable grid size  $\Delta$  and thus subgrid combustion models for LES have to be used.

The aim of this study is to compare different LES combustion models: a Flame-Wrinkling (FW) LES model, (Weller *et al.*, 1997), a Monotone Integrated LES (MILES) model in conjunction with global chemistry modeling, (Grinstein and Kailasanath, 1994), and a Linear Eddy Model (LEM), (e.g. Menon *et al.*, 1993). We first focus on the issue of formulating the reactive flow problem in the framework of LES, and then we describe the most promising LES combustion models presently used. Next we explain the laboratory combustor used for validation and comparison purposes in this investigation (Pitz and Daily, 1983). LES results from non-reactive and reactive flows are then presented, discussed and compared with experimental data. Finally, a discussion is provided that is devoted to the performance and characteristics of the different LES combustion models.

## LES COMBUSTION MODELS

The governing equations of reactive flows are the

Navier-Stokes Equations (NSE) for balance of mass, momentum, energy and species. Simulation of turbulent reacting flows encompasses dealing with a wide range of length and time scales. The largest scales are related to the geometry whilst the smallest are associated with the dissipation of turbulence through viscosity. Chemical reactions have their own spectrum of scales, and a variety of interactions between chemistry and turbulence are possible depending on the overlap of scales. In order to handle this broad spectrum of scales the NSE are low-pass filtered in LES to remove the scales below  $\Delta$ . Applying such a filtering operation to the reactive NSE yields,

$$\begin{cases} \partial_t(\bar{\rho}) + \nabla \cdot (\bar{\rho} \tilde{\mathbf{v}}) = 0 \\ \partial_t(\bar{\rho} \tilde{\mathbf{v}}) + \nabla \cdot (\bar{\rho} \tilde{\mathbf{v}} \otimes \tilde{\mathbf{v}}) = -\nabla \bar{p} + \nabla \cdot (\bar{\mathbf{S}} - \mathbf{B}) + \bar{\rho} \tilde{\mathbf{f}} \\ \partial_t(\bar{\rho} \tilde{\mathbf{h}}) + \nabla \cdot (\bar{\rho} \tilde{\mathbf{v}} \tilde{\mathbf{h}}) = \bar{p} + \bar{\mathbf{S}} \cdot \bar{\mathbf{D}} + \nabla \cdot (\bar{\mathbf{h}} - \mathbf{b}) + \bar{\rho} \tilde{\sigma} \\ \partial_t(\bar{\rho} \tilde{Y}_i) + \nabla \cdot (\bar{\rho} \tilde{\mathbf{v}} \tilde{Y}_i) = \nabla \cdot (\bar{\mathbf{j}}_i - \mathbf{b}_i) + \bar{w}_i \end{cases} \quad (1)$$

where  $\rho$  is the density,  $\mathbf{v}$  the velocity,  $p$  the pressure,  $\mathbf{S}$  the viscous stress tensor,  $\mathbf{f}$  the body force,  $h$  the mixture enthalpy,  $\mathbf{S} \cdot \mathbf{D}$  the viscous work,  $\mathbf{h}$  the heat flux vector,  $\sigma$  the non-mechanical energy supply,  $Y_i$  the species mass fraction,  $\mathbf{j}_i$  the species mass flux vector and  $w_i$  the reaction rate for species  $i$ . Overbars and tildes denote filtering, and density weighted filtering, respectively (cf. Sagaut, 2001). Here,  $\mathbf{f}$  and  $\sigma$  are assumed negligible. The subgrid effects need to be included by means of models for (i) the subgrid momentum, energy and species transport terms  $\mathbf{B}$ ,  $\mathbf{b}$ , and  $\mathbf{b}_i$ ; (ii) the filtered constitutive equations  $\bar{p}$ ,  $\bar{\mathbf{S}}$ ,  $\bar{\mathbf{h}}$ ,  $\bar{\mathbf{j}}_i$  and  $\bar{p}$ ,  $\bar{\mathbf{S}} \cdot \bar{\mathbf{D}}$ ; and (iii) the filtered species reaction rates  $\bar{w}_i$ . The subgrid contributions to the constitutive equations, including the diffusive transport processes, are often neglected, e.g.  $\mathbf{S} \approx \mathbf{S}(\bar{p}, T, Y_j, \nabla \tilde{\mathbf{v}})$ . Moreover, it is usually assumed that  $\bar{\mathbf{S}} \cdot \bar{\mathbf{D}} \approx \bar{\mathbf{S}} \cdot \bar{\mathbf{D}}$  and  $\bar{p} \approx \bar{p}$ . Subgrid models for  $\mathbf{B}$  and  $\mathbf{b}$  are not unique to reactive flows and can hence be selected among the wealth of subgrid models developed for non-reactive flows (cf. Sagaut, 2001). Closure models for  $\mathbf{b}_i$  and  $\bar{w}_i$  therefore constitute the pacing item for LES of reactive flows. Two methods for the closure of these terms can be distinguished: either they are modeled separately, or by combined models.

### The MILES Model

The MILES model (Grinstein and Kailasanath, 1994, Fureby *et al*, 2000) is based on solving the unfiltered reactive NSE for a global reaction mechanism. The thermodynamic model uses the equation of state for an ideal gas mixture and the standard equation of state for the mixture enthalpy. Diffusive transport processes, i.e. viscosity, thermal conduction, molecular diffusion and thermal diffusion are included using species and temperature dependent coefficients. Molecular diffusion is described by a generalized Fickian scheme, the mixture viscosity is modeled by Sutherland's law, thermal conduction is included in a simi-

lar way as the mixture viscosity, whilst thermal diffusion effects are neglected. Finite rate chemistry is included using global two-step mechanisms, with reaction-rates described by Arrhenius models, with coefficients obtained by matching with detailed reaction mechanisms, (Westbrook and Dryer, 1981). The reactive NSE are discretized using a finite volume method, effectively filtering the reactive NSE across the grid, (Fureby & Grinstein, 1999). Time integration is performed with the Crank Nicholson method. Viscous and diffusive terms are treated using central differencing. Convective terms are represented by a Flux Corrected Transport (FCT) scheme, in which the functional reconstruction is performed by hybridizing a low-order dispersion-free flux function with a high-order flux function using a non-linear flux limiter  $\Gamma$ . The limiter  $\Gamma$  is selected as to enforce monotonicity, positivity (when appropriate) and causality, and results in implicit (or built-in) momentum and energy subgrid closure models of generalized eddy-viscosity and eddy-diffusivity form.

### The Flame-Wrinkling Model

The FW-model (Weller *et al.*, 1997, Fureby, 2000), belongs to the class of thin flame models. This concept is widely used due to its simplicity and the fact that the chemical reactions are often confined to thin wrinkled interfaces separating cold reactants and hot products. The FW-model is based on solving the filtered mass, momentum and energy equations (1<sub>1</sub>-1<sub>3</sub>) together with an equation for a reaction coordinate  $b$ , measuring the progress of reaction. This model has been derived using both conditional filtering and traditional low-pass filtering. Independently of method, the transport equation for the resolved part of the reaction coordinate  $\tilde{b}$  takes the same form, having the effective reaction-diffusion imbalance  $\nabla \cdot \bar{\mathbf{j}} - \bar{w}$  represented by the flame-wrinkling density  $\Xi$ , and the unstretched laminar flame speed  $S_u$ , i.e.

$$\partial_t(\bar{\rho} \tilde{b}) + \nabla \cdot (\bar{\rho} \tilde{\mathbf{v}} \tilde{b}) = \nabla \cdot \bar{\mathbf{j}} - \bar{w} = -\rho_u S_u \Xi |\nabla \tilde{b}| \quad (2)$$

An exact transport equation for  $\Xi$  can be derived that is related to the transport equation for the subgrid flame surface density  $\Sigma$ . The generation and removal terms in this equation needs, however, modeling – the approach taken here uses the flame speed correlation of Gülder (1990), which has proven particularly good. Within this framework, a transport equation for  $S_u$  is formulated in which  $S_u$  is advected with the surface averaged interface velocity, affected by chemical and strain-rate time scales, as modeled by asymptotic relaxation. This model requires the unstrained flame speed  $S_u^\infty$ , and the strain response  $\sigma_{ext}$ , both of which may be the result of an analysis of the reactive diffusive structure of the premixed flame. The momentum and energy subgrid closure models are of ordinary eddy-viscosity or diffusivity form whilst the thermodynamics and diffusive trans-

port processes are modeled in the same way as for MILES. The governing equations are here discretized using second order accurate central schemes, and the discretized equations are solved in a sequential manner with the Courant number  $Co < 0.2$ .

### The Linear Eddy Model

LEM was first developed as a stand-alone model for scalar mixing in turbulent flows, but has been shown to be an attractive subgrid model for the reaction-diffusion imbalance, (Chakravarty and Menon, 1999). LEM is a stochastic method which treats molecular diffusion, chemistry and turbulent convection separately but concurrently. The turbulence kinematics is implemented as a Monte-Carlo type method in order to compute statistical properties of scalar fields, such as  $Y_i$  and  $h$  along a one-dimensional, arbitrarily oriented, sub-domain within each LES cell, i.e.,

$$\begin{cases} \partial_t(\rho Y_i) + \partial_s(D_s \partial_s Y_i) = f_i^{\text{stir}} + w_i \\ \partial_t(\rho h) = \partial_s(\kappa \partial_s h) + f_h^{\text{stir}} \end{cases} \quad (3)$$

The thermodynamics and diffusive transport processes are modeled in the same manner as for MILES. Since turbulent convection is implemented explicitly, the convective terms in the species and enthalpy equations are symbolically represented by  $f_i^{\text{stir}}$  and  $f_h^{\text{stir}}$ , respectively. The terms are implemented using stochastic rearrangement events or triplet maps (Menon, 1993) each of which represents the action of the small-scale turbulence on  $Y_i$  and  $h$ . This rearrangement mimics the action of individual eddies on the scalar fields, and is controlled by the characteristic eddy size,  $\lambda$ , and the frequency of the rearrangement. Scaling the diffusivity of a random walk process to the subgrid diffusivity provides sufficient constraints for the determination of  $\lambda$  and its distribution. The chemistry is implemented in (3) in a straightforward manner, as for the MILES model, using a two-step global reaction mechanism, (Westbrook and Dryer, 1981). The LES-equations are here solved using a second order accurate scheme with a Courant-number restriction of  $Co < 0.2$ .

### DESCRIPTION OF THE TEST CASE

An appropriate test case for comparison and validation studies, for which experimental data is available, is the laboratory rig of Pitz and Daily, (1983). This combustor consists of a rectilinear premixing section followed by a smooth contraction to one half of its height, continued by a step expansion into the main combustor that is followed by a section in which cooling water is injected, figure 1. In the experiments a premixed propane-air flame, with an equivalence ratio of  $\phi = 0.57$ , is studied. The pressure, temperature and velocity at the inlet are  $p_0 = 101$  kPa,  $T_0 = 293$  K and  $v_0 = 13$  m/s, respectively, corresponding to a step-height  $Re$  number of  $Re_h = 22 \cdot 10^3$ . Appropriate inflow and outflow boundary conditions (Poinsot and Lele,

1992) are given at the inlet and outlet, respectively, whereas reflecting, adiabatic, no-slip conditions are prescribed at the upper and lower walls. In the spanwise direction, periodic conditions are enforced at a distance of  $3h$  apart. All simulations are initialized with quiescent conditions and the flow evolves naturally. Two grids of  $160 \times 30 \times 60$  and  $320 \times 60 \times 90$  cells, in the streamwise, spanwise and cross-stream directions, respectively, are used. Geometrical progression is here used to improve the spatial resolution of the shear layer and near wall regions.

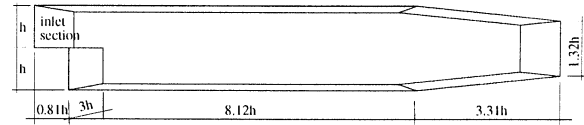


Figure 1: Schematic of the laboratory combustor.

### NON-REACTING FLOW RESULTS

With the intent of providing a better understanding of the flow in general, non-reactive flow simulations were first carried out. Figure 2 shows a perspective view of the vortical flow structures in terms of the vorticity number  $N_k = \|\mathbf{W}\|/\|\mathbf{D}\|$ , where  $\mathbf{W}$  is the rate-of-rotation tensor and  $\mathbf{D}$  is the rate-of-strain tensor, at a level of  $N_k = 1.25$ . In regions with  $N_k > 1$  vorticity dominates over strain, and these regions can thus be interpreted as vortical structures.

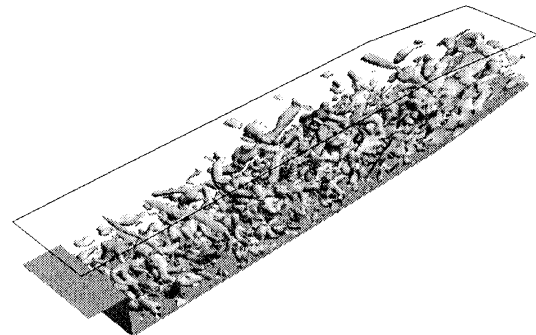


Figure 2: Vorticity distribution in non-reacting flow as illustrated by an iso-surface of  $N_k = 1.25$ .

A laminar, unstable shear layer leaves the step, expands at a short distance from the step and is gradually transformed into a series of roll-up eddies which grow by the distance from the step. The interesting features of this flow is the formation mechanism of these eddies, how they expand as they move downstream, and how this situation is affected by chemical heat release. By investigating animations of e.g.  $N_k$  we conclude that large Coherent Structures (CS) are being formed in a quasi-orderly fashion and carried through the mixing layer, whilst growing by coalescence and engulfment. It is during this process that irrotational fluid is ingested and enfolded into the large CS's. Meanwhile, internal mixing is occurring by the action of small-scale turbulence and viscosity, and the new fluid is digested and incorporat-

ed into the expanding CS. In addition, the spanwise vortices that shed off the step are gradually transformed into longitudinal vortices, mainly by inviscid mechanisms, and a complex vortical pattern follows. The CS's impinge on the lower wall and are either carried away downstream, and transformed into arch-shaped vortices or become trapped in the recirculation bubble. The growth of the CS's (with the distance from the step) affects the recirculation region and thus the rate-of-spread of the shear layer.

Figure 3 shows a typical comparison of the mean streamwise velocity  $\langle v_1 \rangle$  and its rms-fluctuation  $v_1^{\text{rms}}$  between experimental data, LES with the Smagorinsky model (SMG) and the One Equation Eddy Viscosity Model (OEEVM) (cf. Sagaut, 2001) and MILES. In general, good agreement with experimental data is found for the  $\langle v_1 \rangle$ -profiles, although the maximum reverse velocity is somewhat underpredicted as compared to the measurement data. From the  $v_1^{\text{rms}}$ -profiles regions of intense turbulence are found to be confined by the shear layer and spread as the layer widens downstream. At reattachment, the turbulence decreases, and the rms-profiles begin to take on the characteristics of fully developed turbulent channel flow. The position of the peak rms-fluctuation initially coincides with the centreline, but drops towards the lower wall with downstream distance at the same time as the profiles broaden. The peak values of  $v_1^{\text{rms}}$  increase at first due to the formation of large coherent structures, to stabilize around 22% of  $u_0$ , being in good agreement with experimental data. Grid refinement gives virtually no improvement with the exception of better agreement between predicted and measured  $v_1^{\text{rms}}$ -profiles further downstream.

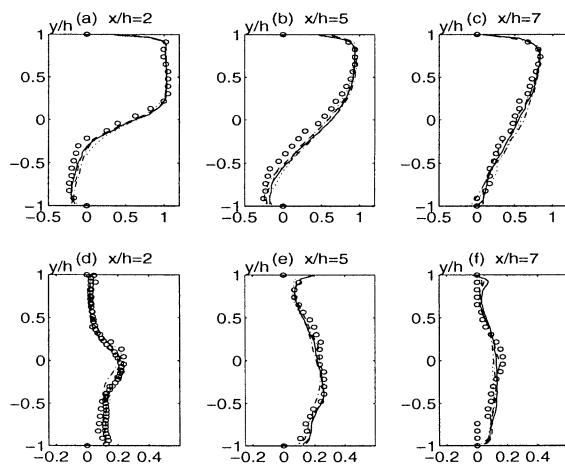


Figure 3: Statistical comparison of  $\langle v_1 \rangle$  and  $v_1^{\text{rms}}$  for non-reacting flow. Legend: (○) Exp. (Pitz and Daily, 1983), (—) SMG, (---) MILES and (- · -) OEEVM.

## REACTING FLOW RESULTS

Some key aspects of the reacting flow are illustrated in figure 4, which presents an experimental schlieren image (figure 4a) and corresponding emulated schli-

eren images from LES with the FW, LEM and MILES models (figures 4b, 4c and 4d), respectively.

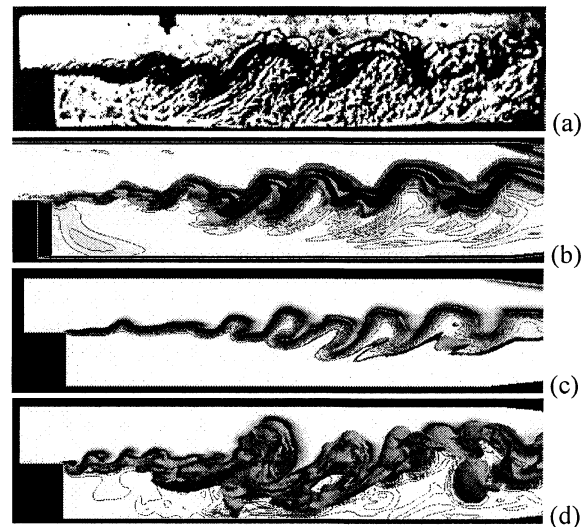


Figure 4: Experimental and emulated schlieren images from turbulent reacting shear layer. Legend: (a) Exp., (b) FW-model, (c) LEM, and (d) MILES.

LES appears successful in capturing the shape and development of the flame, although differences are observed between the different subgrid models. The incoming fluid contains premixed reactants, which mix with hot combustion products in the shear layer, behind the step prior to burning. As for the non-reacting case, CS's are formed in the initially laminar shear layer that shed of the step. These grow by entrainment, heat expansion and coalescence as they move downstream. Due to concentration of vorticity, longitudinal vortices develop together with undulations of a recently shed spanwise vortex in areas of high-strain between subsequent vortices of the same orientation. Based on the shear-layer development it is anticipated that exothermicity occurs mainly within the CS as they entrain cold reactants and hot products, causing volumetric expansion. Volumetric expansion due to exothermicity, baroclinic torque and temperature dependent viscosity effects combine to form thicker vortical structures as compared to the non-reacting flow, hence reducing the strain of the flame and the mass entrainment rate. The longitudinal vortices mainly wrinkle the reaction sheet, and thus, this surface develops regions of high curvature. As the flame is advected downstream it propagates normal to itself at the speed  $S_f$ , causing negatively curved wrinkles to contract, and positively curved wrinkles to expand, this also increases the possibility of pockets of reactants breaking away from the rest of the reactants. As spanwise vortices shed off the step and roll up, cold reactants and hot combustion products become entrained and mix macroscopically. Reaction is, however, initially quenched by the high strain-rate in the shear-layer, causing a cha-

racteristic time delay that is typical of the observed large-scale pattern of burning CS's.

Figure 5 shows a preliminary comparison of the axial mean velocity  $\langle v_1 \rangle$  and its rms-fluctuation  $v_1^{\text{rms}}$  between LES using the FW, LEM and MILES models on the coarse grid and experimental data.

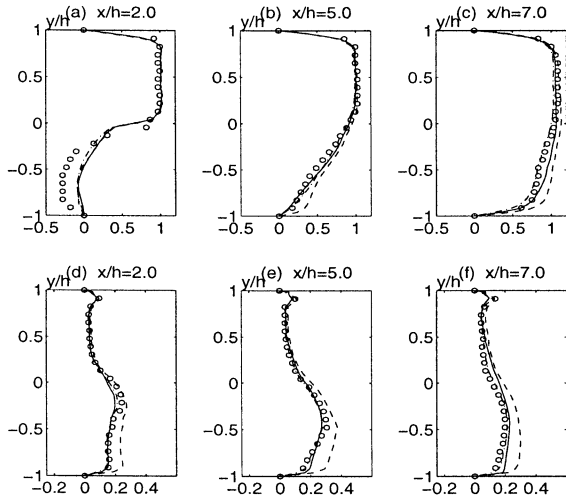


Figure 5: Statistical comparison of  $\langle v_1 \rangle$  and  $v_1^{\text{rms}}$  for reacting flow. Legend: (o) Exp. (Pitz and Daily, 1983), (—) FW, (---) MILES and (- · -) LEM.

The predicted  $\langle v_1 \rangle$ -profiles are in reasonable agreement with the experimental data, with the largest deviations in the recirculation region ( $x_1/h < 6.5 \pm 0.5$ ). Here, all LES underpredict the reverse velocity with about 10%. The reason for this may be that adiabatic no-slip wall boundary conditions are used in LES, whilst the walls of the laboratory rig are cooled. The cooling reduces the heat-release through large-scale mixing, thus increasing the reverse velocity as compared to an adiabatic wall. This will be further studied elsewhere. Comparison of predicted and measured  $v_1^{\text{rms}}$ -profiles shows reasonable agreement, with the best agreement for the FW-model and the least satisfactory for the MILES model, still being within 10% of the data. Regions of intense turbulence are bounded by the shear layer and widens with downstream distance. Near reattachment, the intensity decrease and the  $v_1^{\text{rms}}$ -profiles begin to resemble those of fully developed turbulent channel flow

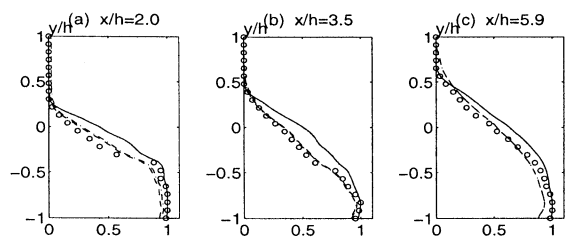


Figure 6. Statistical comparison of  $\langle Y_{\text{CO}_2} \rangle$  for reacting flow. Legend as in figure 5.

Figure 6 presents a comparison of the time aver-

aged  $\text{CO}_2$  mass-fraction  $\langle Y_{\text{CO}_2} \rangle$  between LES using the FW, LEM and MILES models and experimental data. The profiles are normalized by the maximum  $\text{CO}_2$  mass-fraction, which occurs at complete combustion. These profiles reflect the spreading of the shear layer and hence also the progress of reaction. Good agreement between the LES results and the experiments can be observed, with the largest differences occurring for the FW-model.

The growth of the shear-layer is delayed in the reacting case as compared to the non-reacting case. Exothermicity affects the flow development via inviscid volumetric expansion and baroclinic vorticity production mechanisms, as well as through temperature dependent viscous effects (viscosity increases by a factor of about 5 in the hot combustion products over that of the cold reactant mixture); a major role is played by these chemical exothermicity effects directly through thickening of the initial shear layer. In addition, the growth-rate of the shear layer is well reproduced by both LES models ( $\delta = 0.30 \pm 0.03$ , with an experimental value of 0.29). Since the reduction in growth-rate between the non-reacting and the reacting cases is small, effects of the density difference across the shear layer appear counter-balanced by the effects of volumetric expansion.

Investigating the temporal energy spectra (from the FW-model) suggests that the spatial resolution is satisfactory for the cut-off wavenumber to be within the inertial sub-range. For the reacting flow the peak energy is, however, shifted towards smaller scales as a direct consequence of flame-generated turbulence. This emphasises that the resolution requirements of LES become even more severe when chemically reacting flows are considered. Conversely, the demands on the subgrid models increase.

## DISCUSSION

For reacting flow problems of practical interest, simplifications of the fluid dynamics description and the chemical reaction mechanisms are unavoidable. The challenge is to identify optimal sets of modeling ingredients that will allow capturing the dominant reacting flow features in practical simulations. Here, we have compared the Flame-Wrinkling (FW) LES model, a Monotone Integrated LES (MILES) model in conjunction with global chemistry modeling, and the Linear Eddy Model (LEM) for the case of a turbulent reactive mixing layer stabilized behind a rearward facing step, for which detailed data from laboratory experiments are available.

The FW-model is a flamelet-type model for pre-mixed combustion. The model is based on treating the reaction-diffusion imbalance as a product of the flame surface density  $\Sigma = \Xi |\nabla \mathbf{b}|$ , where  $\Xi$  is the flame wrinkling density,  $\rho$ , and the laminar flame speed  $S_{\text{L}}$ . Within the framework of the FW-model, physically-based transport equation, semi-algebraic or al-

gebraic closure models has been developed for these terms. The FW-model therefore has the possibility of handling complex chemistry, through  $S_u$ , and turbulence effects, through  $\Xi$ , separately but concurrently. Furthermore, the FW-model can easily be extended to non-premixed combustion.

The MILES framework provides an effective alternative to conventional subgrid models when seeking improved LES for inhomogeneous flows. Desirable features supporting MILES include: (i) tensorial (anisotropic) nature of the implicitly built-in subgrid model when based on flux limiters (e.g., FCT); (ii) combustion and flow dynamics naturally built-in through functional reconstruction based on physics-based modeling in the time-dependent conservation equations; (iii) reduced competition between subgrid model and discretization errors (i.e. no commutation errors); (iv) inherently simple (unified) implementation for combustion problems involving flame-regions of different character.

The LEM model recognizes the need to resolve all the scales of the problem, and use a one-dimensional, arbitrary oriented, sub-domain for solving the reaction-diffusion problem coupled to subgrid turbulence transport. Hence, small scale turbulent mixing, combustion chemistry and interactions taking place between mixing and reaction is modeled accurately. LEM can be applied to premixed or non-premixed combustion without significant modifications. This aspect differentiates LEM from PDF methods. Splicing transports the full subgrid scalar structure and thus captures gradient and counter-gradient diffusion without additional modeling.

In conclusion, although the examined LES combustion models are different, they produce similar results, which generally are within the uncertainty of the measurement data, taking into account that some issues of the laboratory combustor are not known in full detail. This shows the strength of LES, and that LES, even for such a complicated problem, is not critically dependent on the details of the subgrid model. This suggests that LES, although research is needed to improve the physics-based modeling, is sufficiently mature to be used in some engineering applications, and that the LES provides more details of the flow than RANS can provide.

## References

Bray, K.N.C. and Libby P.A., 1994, "Recent Developments in the BML Model of Premixed Turbulent Combustion", in *Turbulent Reacting Flow* (eds. Libby P.A. and Williams F.A.), Academic Press.

Chakravarthy, V.K. and Menon, S., 1999, "Modeling of Turbulent Premixed Flames in the Flamelet Regime", In *Proceedings of First Symp. on Turbulence and Shear Flow Phenomena*.

Dopazo, C., 1994, "Recent Developments in PDF Methods", in *Turbulent Reacting Flows*, Ed. Libby P.A. and Williams F.A., Academic Press.

Fureby, C. and Grinstein, F.F., 1999, "Monotonically Integrated Large Eddy Simulation of Free Shear Flows", *AIAA.J.*, vol. 37 p 544.

Fureby, C., 2000, "Large Eddy Simulation of Combustion Instabilities in a Jet Engine Afterburner Model", *Comb. Sci. and Tech.*, vol. 161, p 213.

Fureby, C., Grinstein, F.F. and Kailasanath, K., 2000, "Large Eddy Simulation of Premixed Turbulent Flow in a Rearward-Facing-Step Combustor", AIAA Paper 00-0863.

Grinstein, F.F. and Kailasanath, K.K., 1995, "Three Dimensional Numerical Simulations of Unsteady Reactive Square Jets", *Comb. and Flame*, vol. 100, p. 2, and vol. 101, p. 192.

Gülder, Ö.L., 1990, "Turbulent Premixed Flame Propagation Models for Different Combustion Regimes", *23rd Int. Symp. on Comb.*, The Combustion Institute, Pittsburgh, USA, p 743.

Jones, W.P., 1993, "Turbulence Modeling and Numerical Solution Methods for Variable Density and Combusting Flows", in *Turbulent Reacting Flows* (eds. Libby P.A. and Williams F.A.), Academic Press.

Menon, S., McMurtry P. and Kerstein, A.R., 1993, "A Linear Eddy Mixing Model for Large Eddy Simulation of Turbulent Combustion", in *LES of Complex Engineering and Geophysical Flows* (eds. Galperin B. and Orszag S.), Cambridge University Press.

Pitz, R.W. and Daily, J.W., 1983, "Experimental Study of Combustion in a Turbulent Free Shear Layer Formed at a Rearward Facing Step", *AIAA J.* vol. 21, p 1565.

Poinsot, T. and Lele, S.K., 1992, "Boundary Conditions for Direct Simulation of Compressible Viscous Reacting Flows", *J. Comp. Phys.*, vol. 101, p 104.

Pope, S.B., 1985, "PDF Method for Turbulent Reacting Flows", *Comb. Sci. and Tech.*, vol. 11, p 119.

Kollmann, W., 1990, "The PDF Approach to Turbulent Flow", *J. Theor. and Comp. Fluid Dyn.*, vol. 1, p 249.

Sagaut, P., 2001, "Large Eddy Simulation for Incompressible Flows", Springer Verlag, Berlin.

Smith, T. and Menon, S., 1992, "Subgrid Combustion Modeling for Premixed Turbulent Reacting Flows", AIAA Paper No 98-0242.

Weller, H.G., Tabor, G., Gosman, D. and Fureby, C., 1997, "Application of a Flame-Wrinkling LES Combustion Model to a Turbulent Mixing Layer", *27th Int. Symp. on Comb.*, The Combustion Institute, Pittsburgh, USA, p 899.

Westbrook, C. and Dryer, F., 1981, "Simplified Reaction Mechanisms for the Oxidation of Hydrocarbon Fuels in Flames", *Comb. Sci. and Tech.*, vol. 27, p 31.